The Effect of Frequency on the Elevated Temperature Fatigue of a Nickel-Base Superalloy

F. E. ORGAN AND M. GELL

In this investigation, the effect of a frequency variation between 2 cpm and 6×10^4 cpm on the 1400°F fatigue properties of wrought Udimet 700 was determined at a constant stress range of 85 ksi. It was found that a peak existed in the cyclic life vs frequency curve such that a) an increase in frequency from 2 to 600 cpm increased the fatigue life 100 times and b) an increase in frequency from 600 to 6×10^4 cpm reduced the fatigue life sevenfold. The peak in the cyclic life vs frequency curve is the result of two competing processes: 1) there is a reduction in the effects of creep and oxidation with increased frequency that tends to increase the life and 2) there is an increase in the heterogeneity of deformation with increased frequency that tends to reduce the life. At low frequencies, crack initiation occurred at surface-connected grain boundaries. Crack propagation was initially intergranular and then proceeded noncrystallographically normal to the stress axis (Stage II mode). Crack initiation at high frequencies occurred at subsurface brittle phases located at grain boundaries or at the intersection of coherent annealing twin boundaries. Crack propagation was entirely transgranular, proceeding initially along twin boundaries or slip bands (Stage I mode) and then changing to the Stage II mode. The statistical nature of the fracture process, the significance of subsurface crack initiation, and the relation of these results to existing high temperature fatigue models are discussed.

NICKEL-BASE superalloys and other high temperature alloys used in gas turbine engines are subjected to fatigue stresses applied over a wide range of frequencies varying from the high vibrational frequencies experienced by turbine blades ($\sim 2.5 \times 10^5$ cpm) to low frequencies associated with the period of engine operation (1 cycle per flight). Although a general awareness of the importance of frequency effects in elevated temperature fatigue has developed in the last few years, the magnitude of the effect and the mechanisms involved are largely unknown.

A good review of work through 1958 on the effect of frequency on a wide range of materials was presented by Stephenson.[1] It was shown that cyclic frequency had little effect on most metals at room temperature, but that at elevated temperatures fatigue life increased with increasing frequency. This increase in life has been attributed to the reduced importance of the creep component in the fatigue cycle.

More recently, several examinations of the effect of frequency on fatigue behavior of nickel-base superalloys at elevated temperatures have been conducted. Tilly[2] found that for Nimonic 90 tested at temperatures above 1112°F (600°C), the fatigue life increased with increasing frequency between 0.1 and 8000 cpm, and increasing frequency favored transgranular compared to intergranular crack propagation. For Nimonic 90 at 1292°F (700°C), Northwood *et al.*[3] found fatigue life increased as frequency was increased from 4400 to 8600 cpm and that the crack leading to failure initiated within the specimen interior.

A number of phenomenological models have been developed that consider the effect of frequency on fatigue life. Eckel[4] and more recently Coles *et al.*[5] have used the equation:

$$\nu^k t = C_1$$

to evaluate the relative influence of creep and fatigue, where ν is the frequency, t is the time and k and C_1 are constants that depend on the material and testing conditions. If $k = 0$, the test is time-dependent, as in pure creep, and if $k = 1$, the test is cycle dependent, as in pure fatigue. For most materials tested at elevated temperatures, k is between 0 and 1, in agreement with observations that the number of cycles to failure generally increases with frequency.

Coffin[6] has developed the concept of a frequency-modified life in order to extend use of the Manson-Coffin equation:

$$\Delta\epsilon_p N_f = C_2$$

to elevated temperatures, where $\Delta\epsilon_p$ is the plastic strain range, N_f the number of cycles to failure and C_2 a constant. The frequency-modified equation is:

$$\Delta\epsilon_p N_f \nu^{k-1} = C_3$$

which is in agreement with some elevated temperature fatigue data. More recently an equation has been developed that relates total strain range, frequency and cyclic life.[7]

Manson *et al.*[8] have recently proposed a linear creep-fatigue damage rule in which the fatigue damage is calculated by the method of universal slopes[9] and the creep damage is determined by running cyclic creep-rupture tests at various stress levels. The creep damage per cycle is then obtained from the cyclic work hardening characteristics of the alloy and the results of the cyclic creep-rupture tests. The effect of frequency is to change the cyclic work hardening or softening characteristics and therefore the amount of creep per cycle.

The phenomenological models for high temperature fatigue that have been developed to date do not consider the actual crack initiation and propagation behavior of materials and how this behavior is modified by time- and temperature-dependent processes. The

F. E. ORGAN and M. GELL are associated with the Materials Engineering and Research Laboratory, Pratt & Whitney Aircraft, Middletown, Conn.

Manuscript submitted August 12, 1970.

Fig. 1—Microstructure of the Udimet 700 alloy. Magnification 160 times.

Table I. Chemical Composition

Element	Nominal Composition
C	0.07
Mn	0.15 max.
S	0.015 max.
Si	0.20 Max.
Cr	15.0
Co	18.5
Mo	5.0
Ti	3.0
Al	4.25
B	0.030
Ni	Remainder

purpose of this study is to provide some of this information as well as to determine the magnitude of the frequency effect.

EXPERIMENTAL PROCEDURE

The material investigated was wrought polycrystalline Udimet 700 supplied in three heats having compositions which corresponded closely with the nominal composition of the alloy (Table I). The standard four-step heat treatment of 4 hr at 2140°F, 4 hr at 1975°F, 24 hr at 1550°F, and 16 hr at 1400°F was applied. The resulting microstructure consisted of grains with an average diameter of 0.006 in. as well as much smaller grains associated with strings of carbides lying parallel to the rolling direction, Fig. 1.

Tests were conducted in air at 1400°F at a mean stress of 47.5 ksi and an alternating stress of 42.5 ksi over a frequency range varying from 2 to 60,000 cpm. Two types of specimens were used: 1) a button-head axial fatigue specimen for tests at 60,000 cpm, Fig. 2(a) and 2) a flat-end axial fatigue specimen for tests at frequencies between 2 and 600 cpm, Fig. 2(b). The specimens were mechanically polished to remove a minimum of 0.002 in. from the gage diameter and then electropolished to remove the traces of mechanical polishing.

Tests between 2 and 600 cpm were conducted on a closed-loop hydraulic fatigue testing machine operated under load control. Temperature was maintained by a

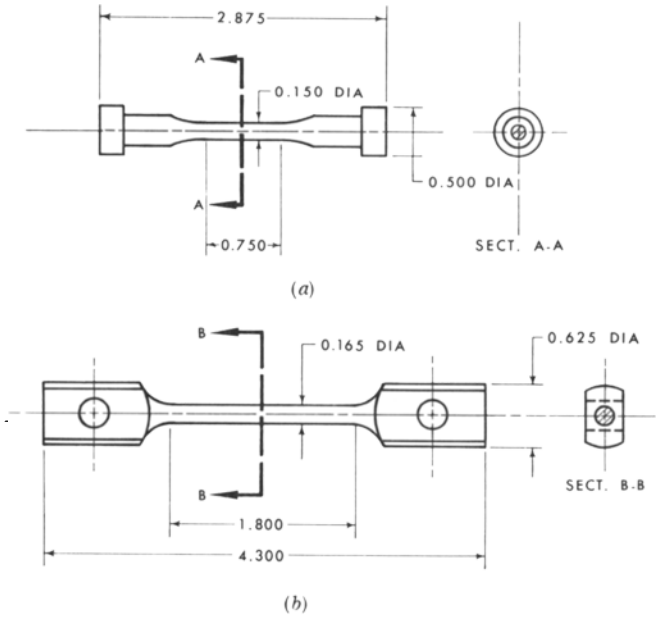

Fig. 2—Specimen design for tests at (*a*) 60,000 cpm and at (*b*) 2 to 600 cpm.

three zone resistance furnace and controlled within ±2°F over the gage section. The 60,000 cpm specimens were tested on a high-frequency electromagnetic oscillator with a static preload. Dynamic loads applied to the specimen are monitored by a load cell permanently fixed in the loading column. Before and after each test the load cell readings were calibrated against the load readings of a strain gaged specimen that was identical to the one being tested. Heating was done with an induction coil and the temperature was maintained within ±10°F by optical pyrometry. All specimens were heated for 1 hr prior to testing to assure uniform temperature distribution throughout the gage section. A sinusoidal wave form was employed for all tests.

EXPERIMENTAL RESULTS

Fatigue Properties

The results of the fatigue tests for a range of frequencies from 2 cpm to 60,000 cpm are presented in Table II and Figs. 3 and 4. Table II also summarizes the metallographic observations of crack initiation and propagation. The fatigue life in cycles increases with increasing frequency to a peak at about 600 cpm and then decreases as the frequency is increased to 60,000 cpm, Fig. 3. The maximum fatigue life observed at 600 cpm was over two million cycles. As the frequency was decreased to 2 cpm, the fatigue life decreased 100 times to 20,000 cycles, and as the frequency was increased to 60,000 cpm, the fatigue life decreased 7 times to 300,000 cycles. The time to failure initially increases with frequency and then declines, Fig. 4. The two data points at 600 cpm showing very low lives in Figs. 3 and 4 will be considered later.

Crack Initiation

Examination of the fracture surface of each specimen cycled at 2 cpm indicated that crack initiation occurred intergranularly at the external surface, Fig. 5. This ob-

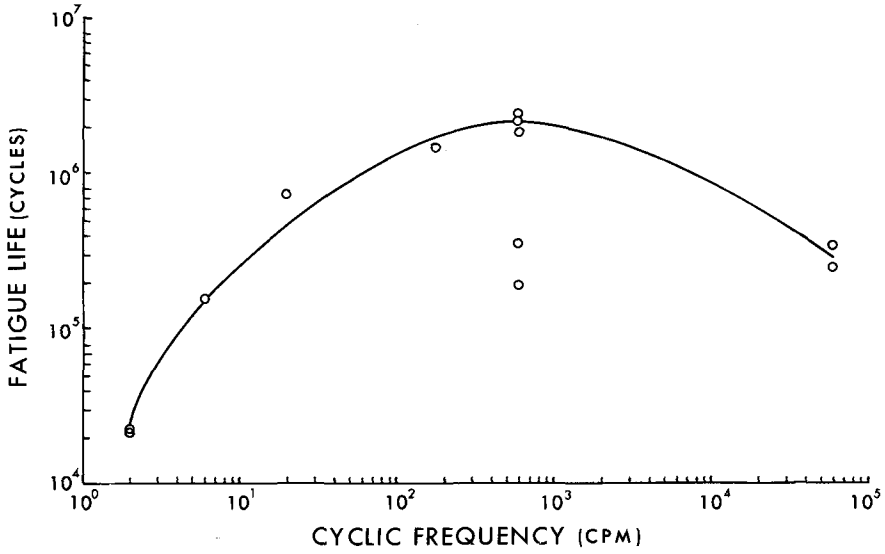

Fig. 3—The effect of frequency on the number of cycles to failure of U-700 at 1400°F and a stress range of 85 ksi.

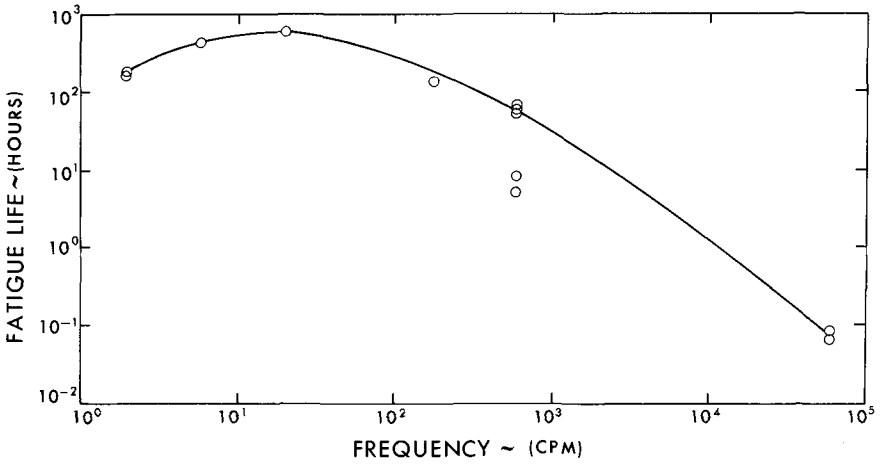

Fig. 4—The effect of frequency on the time for failure of U-700 cycled at 1400°F and a stress range of 85 ksi.

Table II. Effect of Frequency on Fatigue Properties of U-700 at 1400°F

Specimen Designation	Frequency, cpm	Fatigue Life, hr	Fatigue Life, cycles	Type of Initiation Site	Mode of Crack Propagation
FV1	2	167	2.20×10^4	Surface intergranular	Intergranular, changing to transgranular Stage II at about three grain diameters below surface.
FV6	2	176	2.10×10^4	Surface intergranular	Intergranular, changing to transgranular at one grain diameter below surface.
FV13	6	439	1.55×10^5	Surface intergranular	Intergranular, changing to Stage II transgranular at about two grain diameters below surface.
FV11	20	622	7.47×10^5	Surface intergranular	Intergranular, changing to Stage II transgranular at about three grain diameters below surface.
FV10	180	137	1.44×10^6	Interior grain boundary	Stage I near initiation site then changes to Stage II, mostly Stage II.
FV2	600	52	1.80×10^6	Interior grain boundary	Stage I near initiation site then changes to Stage II, mostly Stage II.
FV7	600	61	2.13×10^6	Interior grain boundary	Stage I near initiation site then changes to Stage II, mostly Stage II.
FV8	600	68	2.40×10^6	Interior grain boundary	Stage I near initiation site then changes to Stage II, mostly Stage II.
FV5	600	8	3.47×10^5	Interior twin intersection	Stage I near initiation site then changes to Stage II, mostly Stage II.
JJ1	600	5.2	1.88×10^5	Interior twin intersection	Stage I near initiation site then changes to Stage II, mostly Stage II.
FV3	60,000	0.07	2.40×10^5	Interior twin intersection	Stage I near initiation site then changes to Stage II, mostly Stage II.
FV9	60,000	0.09	3.31×10^5	Secondary initiation site: interior grain boundary	Stage I near initiation site then changes to Stage II, mostly Stage II.

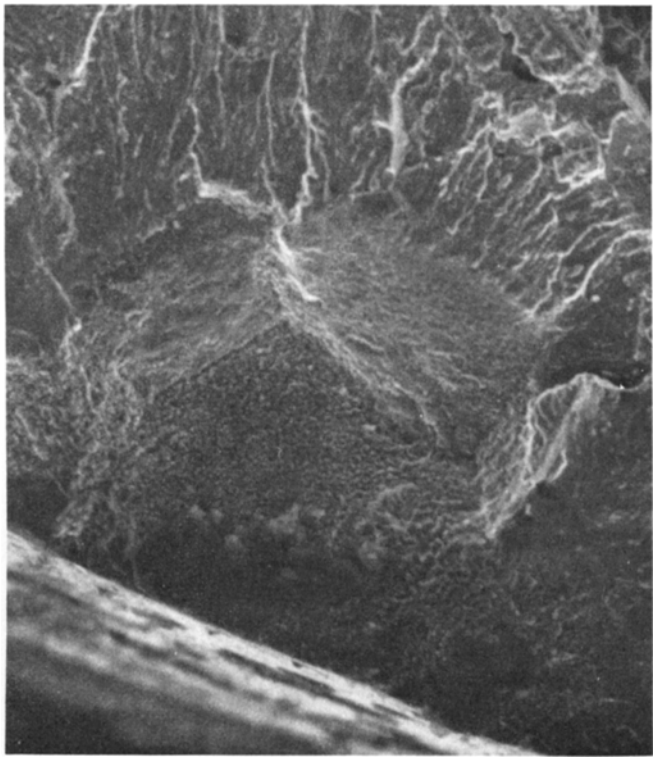

Fig. 5—The fracture surface of a 2 cpm specimen showing intergranular cracking adjacent to the specimen surface (bottom) and transgranular Stage II cracking further away (top), scanning electron micrograph. Magnification 320 times.

servation was confirmed by taking longitudinal sections through the specimens which showed intergranular secondary cracks extending from the surface on all surface-connected grain boundaries, Fig. 6(*a*). Oxidation of these surface-connected cracks resulted in widening of the crack and depletion of the γ' precipitate around the crack. No secondary cracks were observed to initiate transgranularly. No internal secondary cracks or cavities were observed based on examination of a large number of longitudinal sections and electron microscope replicas prepared from these sections. Failure in the specimens tested at 6 and 20 cpm also originated at surface-connected grain boundaries.

The initiation site for failure of the 180 cpm specimen and for each of the 600 cpm specimens lasting 2 million cycles was at a subsurface grain boundary. Examination of a 600 cpm specimen (FV2) by scanning electron microscopy showed the initiation site to be at the interface of a particle located at a grain boundary, Fig. 7. The crack does not propagage along the grain boundary but immediately proceeds along $\{111\}$ planes in two grains and in the Stage II mode in the third grain (upper right). The grain boundary containing the initiation site was generally free of precipitate in contrast to most grain boundaries in the material. Further investigation of the Udimet 700 microstructure showed that a small number of grain boundaries did not have a continuous chain of particles. The absence of particles sometimes corresponded to locations where a coherent annealing twin intersected a grain boundary as in Fig. 8, but this was not generally the case.

The initiation site for the crack leading to failure for each short-lived 600 cpm specimen (FV5, JJI) was found to be at the intersection of two coherent annealing

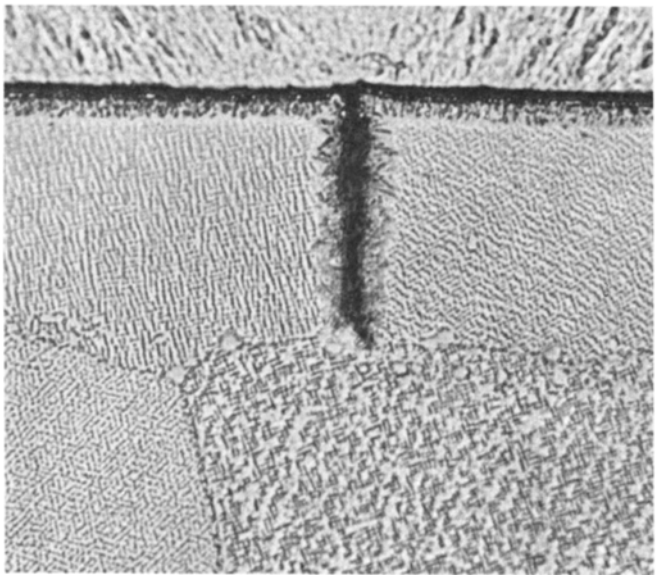

(*a*)

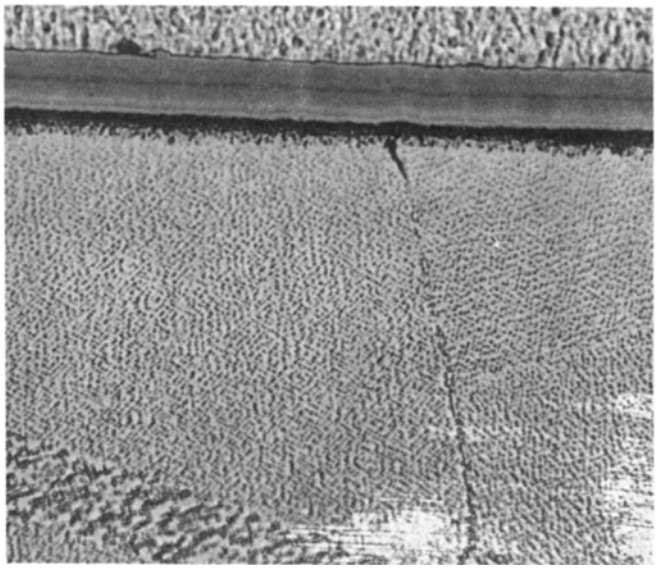

(*b*)

Fig. 6—Surface-connected intergranular cracking at (*a*) 2 cpm, showing oxide within and adjacent to the crack and at (*b*) 600 cpm, where the intergranular cracks are very short. Magnification 1,250 times.

twin boundaries within a single subsurface grain. Examination by scanning electron microscopy of FV5 showed that a particle was near the initiation site, Fig. 9. Electron probe analysis revealed a high titanium content in the particle. The chemical analysis and the shape of the particle indicate it is probably TiC. Although the precipitation of hard brittle phases at twin intersections was unusual, a few additional cases were observed. More frequently, chains of particles similar to those at grain boundaries were found along twin boundaries, Fig. 10, and even more often along incoherent twin boundaries.

Secondary cracking in all specimens cycled at 600 cpm was observed at some surface-connected grain boundaries but extended at most $\frac{1}{10}$ grain diam below the surface, Fig. 6(*b*). No other secondary cracking was observed.

(*a*)

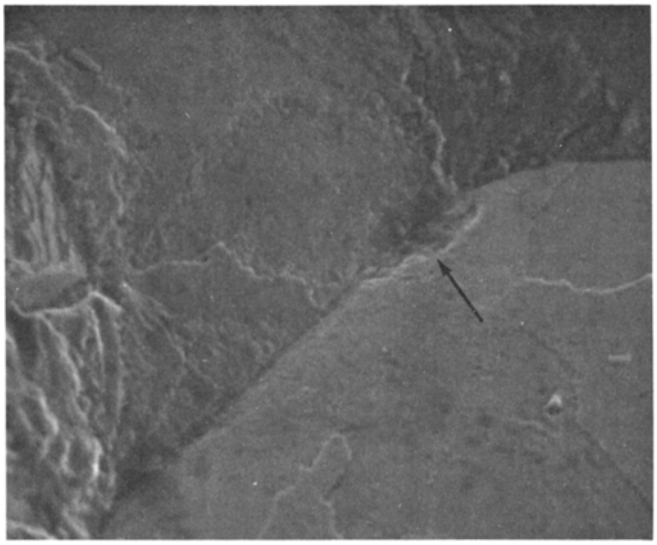

(*b*)

Fig. 7—Fracture surface of a 600 cpm specimen showing subsurface fracture origins at the interface of a particle in a grain boundary, arrow (particle is missing). Stage I crack propagation occurs toward the top left and bottom right and Stage II toward the top right. Scanning electron micrographs. (*a*) Magnification 280 times, (*b*) magnification 130 times.

Examination of the two 60,000 cpm specimens indicated crack initiation at a twin intersection in one case and at a grain boundary in the other case. The initiation site in specimen FV3 was a particle at the intersection of two twins, Fig. 11. The particle was found to be high in molybdenum content and is possibly Mo_3B_2. The primary initiation site for specimen FV9 could not be determined. However, a secondary initiation site of FV9 and the initiation site of a specimen cycled to a maximum stress 5 pct below the specified stress (not shown in Table II) exhibited grain boundary initiation.

Crack Propagation

Crack propagation at 2, 6, and 20 cpm began in an intergranular mode from a surface initiation site. The crack extended intergranularly along the surface and to a depth of 1 to 3 grain diam below the surface on grain boundaries approximately normal to the stress axis before changing to the transgranular Stage II mode of crack propagation. Many secondary intergranular cracks were observed to have stopped or changed to the Stage II mode at grain boundary triple points, Fig. 12. Two regions of Stage II propagation, similar to those observed by Ellison and Sullivan[10] covered the remainder of the fatigue portion of the fracture surface. The Stage II region nearest the initiation site was very flat whereas the region near the overload zone had a much rougher topography. River lines were found in both regions and striations were observed in the second region. At the perimeter of the fatigue zone several highly reflective crystallographic facets oriented approximately 60 to 70 degrees to the stress axis were observed to contain widely-spaced striations, Fig. 13. Laue X-ray back-reflection photographs showed these facets to be $\{111\}$ planes.

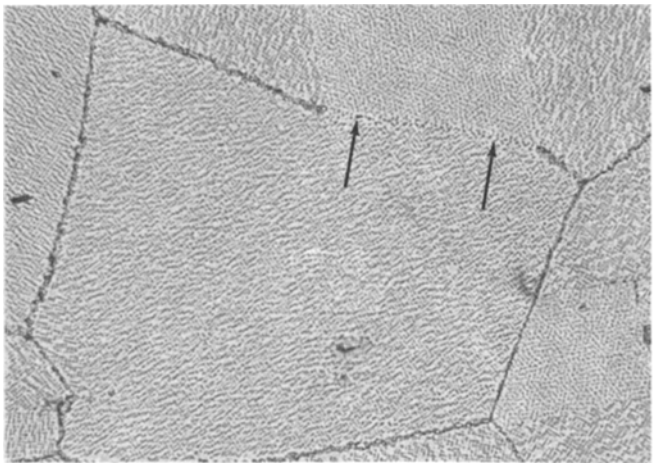

Fig. 8—Microstructure of U-700 showing a grain boundary region devoid of $M_{23}C_6$ precipitate (arrows). Magnification 800 times.

The fracture surfaces of the specimens cycled at 180, 600, and 60,000 cpm were similar to one another. In each case, crack propagation began in the Stage I transgranular mode and extended a maximum of 3 grain diam from the initiation site before changing to the Stage II mode, Figs. 7, 9, and 11. There is generally a slightly larger Stage I zone in the 60,000 cpm specimens and for one 60,000 cpm test run at a stress about 5 pct below the other tests, crack propagation was entirely Stage I. River lines and fracture steps associated with Stage I fatigue fracture[11] were observed on some Stage I facets while other facets showed no markings. The Stage II region was similar to that in the two cpm specimens in that it consisted of a relatively flat zone near the Stage I region and a rougher zone near the overload region, although the boundary of these zones was not as well-defined as for the two cpm specimens. Occasionally, a small intergranular region was observed within the Stage II region due to a suitably oriented grain boundary. Stage I facets were observed at the end of the Stage II region near the overload zone on some 600 and 60,000 cpm specimens. The fatigue crack broke through the surface before the onset of tensile overload failure in the 180 and 60,000 cpm specimens, but failure occurred before the crack reached the surface for each test at 600 cpm.

DISCUSSION

The results have shown that both the cyclic life and the time to failure first increase, reach a peak and then decrease with increased frequency, Figs. 3 and 4. Low frequencies favor surface intergranular crack initiation and intergranular crack propagation. High frequencies favor subsurface initiation at grain boundaries and twin boundary intersections, and transgranular crack propagation.

At low frequencies cracking starts at each surface-connected grain boundary, but there is no indication of subsurface cracking. Preferential intergranular oxidation occurs because of the presence of $Cr_{23}C_6$ and other brittle phases having poor oxidation resistance in grain boundaries and because of accelerated oxygen diffusion along the boundaries. The oxide in the boundary is poorly bonded to the matrix and serves as an easy site for cracking. It can be considered that above a specific oxide thickness, the oxide layer serves as a notch of depth equal to the oxide thickness. Thus as the cyclic frequency is increased, it should require about the same time and therefore a greater number of cycles to initiate an intergranular crack. If this were the only operative time-dependent mechanism, then the time to failure at low frequencies would be expected to be constant. However, as Fig. 4 shows, the time to failure initially increases with frequency. This indicates that a second time-dependent fracture mechanism operates at the lowest frequencies and then ceases as the frequency increases. This mechanism is believed to be creep deformation, which is more extensive in the 2 cpm specimen compared to that cycled at 20 cpm despite the shorter life of the former, Fig. 14. No evidence for permanent creep damage such as cavitation or subsurface cracking was observed.

As the frequency is increased above 20 cpm, the amount of creep deformation decreases and intergranular oxidation ceases to be of importance as a determinant of fatigue life as evidenced by the subsurface location of the crack initiation site. Correspondingly, the cycles to failure increase. Eventually a peak is reached in the cyclic life and then the cyclic life is reduced with increased frequency. This rather unusual result can be explained by the slip character and cracking mode of this class of materials.

The initial mode of crack propagation is Stage I for specimens tested on both sides of the peak in life. Stage I cracking has been described as a slip plane decohesion process that is dependent on the generation of planar slip bands at the crack tip.[12,13] More recently it has been found that the more homogeneous distribution of planar slip at 1400°F compared to that at room temperature in a single crystal alloy can account for the improved endurance limit at the higher temperature.[14] Likewise it has been shown that increased frequency is similar to reduced temperature in favoring heterogeneously-distributed planar slip and Stage I cracking.[13-15] A reduced homogeneity of deformation with increased frequency has also been observed in copper,[16,17] alpha-brass,[17] and iron,[18] and in the latter case leads to a reduced fatigue limit. Based on these observations, it is concluded that the reduced fatigue

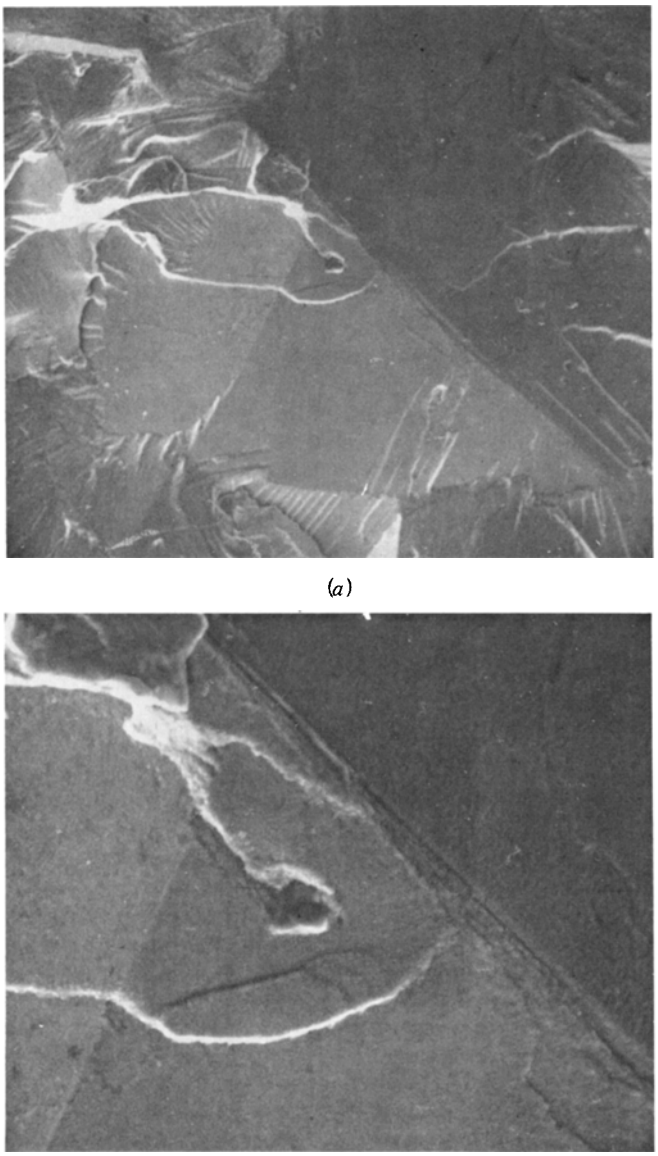

(a)

(b)

Fig. 9—Fracture surface of a 600 cpm specimen showing subsurface fracture origin at the intersection of coherent annealing twins within a grain. A particle thought to be TiC is near the initiation site. Stage I crack propagation occurs until the grain boundary is reached. Scanning electron micrographs. (a) Magnification 280 times, (b) magnification 930 times.

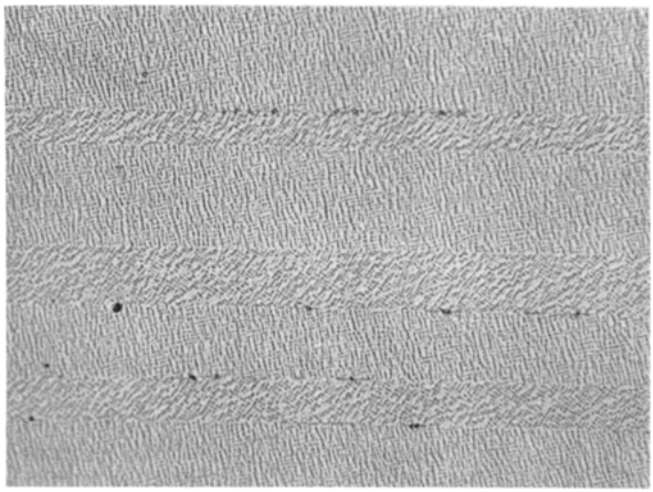

Fig. 10—Precipitates along coherent annealing twin boundaries. Magnification 790 times.

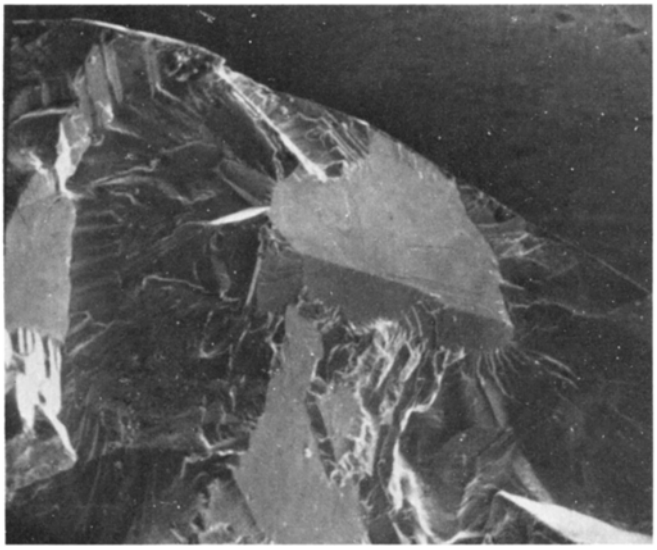

(a)

(b)

Fig. 11—Fracture surface of a 60,000 cpm specimen showing subsurface fracture origin at a particle (arrow) located at the intersection of coherent annealing twins. Crack propagation is initially in the Stage I mode. Scanning electron micrographs. (*a*) Magnification 93 times, (*b*) Magnification 930 times.

life with increased frequency above 600 cpm can be attributed to the increased strain within a fewer number of slip bands. Under these circumstances the number of cycles to crack initiation are reduced and the rate of Stage I crack growth is increased. At lower frequencies, thermally-activated processes such as dislocation climb and cross slip which lead to homogeneous deformation can occur and the fatigue life is correspondingly increased. Slip band etching techniques and thin foil transmission electron microscope observations were not able to substantiate this concept because, with the test conditions employed, high frequency deformation is limited and restricted to the periphery of microstructural defects and cracks. However, it has been shown that elevated temperature tensile deformation in nickel-base superalloys becomes more homogeneous as strain rate is reduced.[15]

In recent tests conducted to determine the effect of

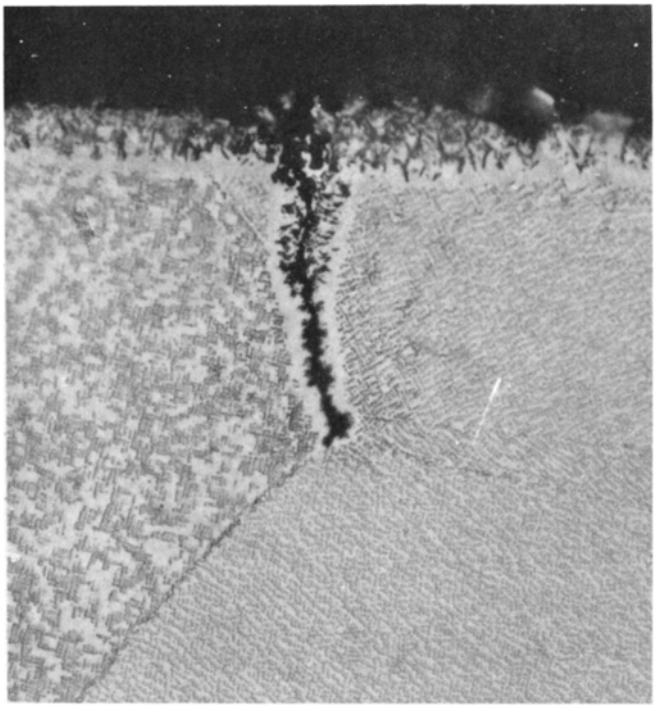

(a)

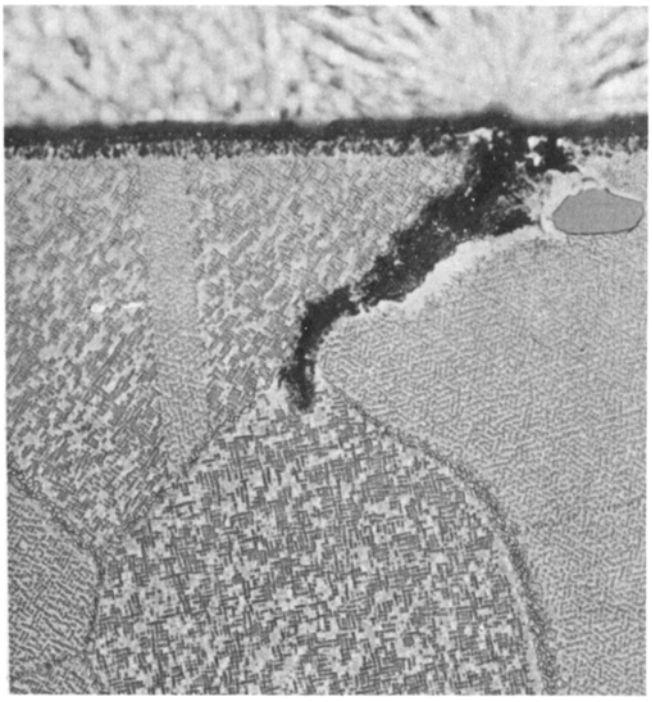

(b)

Fig. 12—Surface-connected intergranular cracks in 20 cpm specimen (*a*) crack stopped at grain boundary triple point. Magnification 1075 times, (*b*) Stage II crack propagation initiated at triple point. Magnification 1075 times.

frequency on single crystal nickel-base superalloys at elevated temperatures,[14] similar behavior to that shown in Fig. 3 was found at 1550°F. These tests support the general nature of the maximum in the curve of fatigue lives vs frequency, at least for this class of materials. In addition, as a result of the single crystal work, this behavior cannot be attributed solely to the

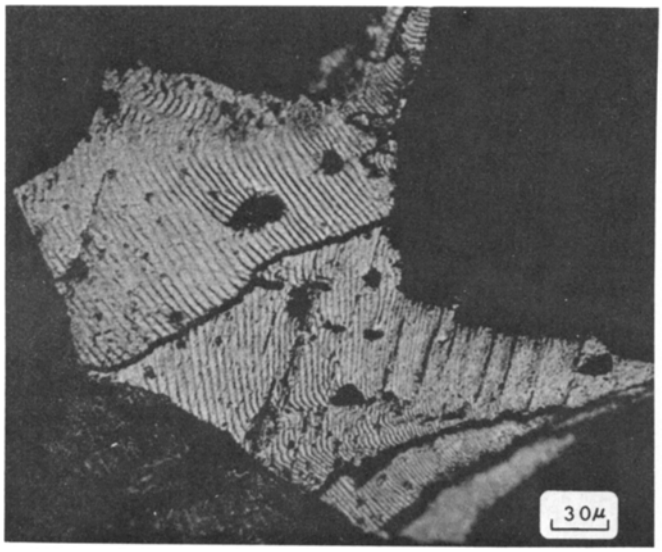

Fig. 13—Crystallographic fracture facet produced by Stage II fracture process. Magnification 245 times.

effect of frequency on intergranular deformation and fracture processes. This study also showed that an increase in temperature to 1700°F shifted the N_f-frequency curve downward and to the right so that there was a continuous increase in life with frequency over the frequency range studied. Likewise, a reduction in temperature to 1400°F shifted the curve upward and to the left so that there was a continuous decrease in life with frequency.

The importance of strain concentration in localized bands on fatigue life can also be seen in the greatly reduced fatigue life of the 600 cpm specimens for which crack initiation occurred at twin intersections within a single grain and crack propagation was along coherent annealing twin boundaries. Crack initiation occurred at a hard brittle particle in the boundary, and Fig. 15 shows that deformation is preferentially concentrated along a twin-matrix interface. This localization of deformation at the twin-matrix interface, which may result from a lower critical resolved shear stress along the boundary plane,[19] results in a reduced fatigue life compared to those 600 cpm specimens in which crack initiation is intergranular, Table II. It should be noted that the low life specimens at 600 cpm at 1400°F have about the same lives as the 60,000 cpm specimens at 1400°F and the 600 cpm specimens at room temperature, Table III. It is proposed that in all three cases, slip dispersal is minimal, Stage I cracking occurs and therefore the lives are similar.

There was no observable difference in the fracture surfaces of the 600 cpm specimens lasting 3×10^5 cycles and those lasting 2×10^6 cycles except for the different initiation site. This suggests that the number of cycles spent in propagation was similar in the two cases and had to be less than 3×10^5 cycles. Thus, most of the difference in life as a function of frequency above 180 cpm can be attributed to crack initiation.

The fracture process and the fatigue life at the higher frequencies is statistical in nature and depends on the presence or absence of favorably oriented microstructural defects. Fracture will occur first at a particle at the intersection of twins within a single grain. Yet not every specimen may contain favorably oriented

(a)

(b)

Fig. 14—Dislocation substructure found in specimens cycled to failure at (*a*) 2 cpm and (*b*) at 20 cpm. Magnification 30,000 times.

twin boundaries. If not, then fracture initiates after a considerably greater number of cycles along a favorably oriented grain boundary which is free of $M_{23}C_6$ precipitate and contains an MC carbide or a boride. If the standard heat treatment employed for this material was successful in providing a uniform distribution of $M_{23}C_6$ on all grain boundaries, then a further improvement in fatigue life would be expected.

The fracture initiation site is below the specimen surface for all tests run above 180 cpm despite initiation of surface-connected intergranular cracks. Subsurface crack initiation has also been observed in elevated temperature tests on single crystal nickel-

Fig. 15—Concentration of plastic deformation in coherent annealing twin boundary (arrows). Magnification 27,500 times.

Table III. Fatigue Life of Polycrystalline Udimet 700 at Stress Range of 85 ksi

Temperature, °F	Frequency, cpm	Cycles to Failure	Mode of Crack Initiation
70[21]	6×10^2	2×10^5	twin band
1400	6×10^2	2×10^6	grain boundary
1400	6×10^4	3×10^5	grain boundary or twin boundary intersection

base superalloys but, in that case, no surface-connected secondary cracking occurred.[13] In contrast both polycrystalline Udimet 700 and the single crystal nickel-base superalloys exhibit crack initiation at the specimen surface at room temperature.[12,19] Since no surface-connected secondary cracking was observed for the single crystals tested at elevated temperatures it was possible to conclude that oxidation retards crack initiation. In a similar manner, it is likely in polycrystalline Udimet 700 that oxidation initially suppresses crack initiation until the size of the intergranular oxide zone reaches a critical size for crack initiation. By that time large cracks have formed in the specimen interior and one of these propagates to failure.

{111} fracture facets exhibiting two distinctly different types of appearance have been observed. The first type of crystallographic cracking occurs at small crack lengths on {111} planes that have a high resolved shear stress. These fracture facets are highly reflective and are either featureless or contain fracture steps and river lines; they do not contain striations. This appearance is typical of Stage I fracture produced in high-cycle fatigue of nickel-base superalloys.[11] As the crack length increases, there is a transition to Stage II cracking on noncrystallographic surfaces approximately normal to the stress axis. At still larger crack lengths, cracking is still predominantly in the noncrystallographic Stage II mode, but cracking is observed on a few {111} facets. These facets contain well-defined striations but there are no river lines, Fig. 13. The facets are usually oriented at 60 to 70 degrees to the stress axis and thus have both a small shear stress and a large normal stress operating. Since the stress intensity factor at the crack tip is large for large crack lengths, deformation can occur both on {111} planes parallel to the crack and on those making a steep angle to the crack plane.[20] The out-of-plane shear displacements give rise to the striations and because of the strain concentration on planes parallel to the crack, fracture occurs on this plane, rather than noncrystallographically. We have then an example of crystallographic Stage II fracture.

The results of this study bear on the assumptions that are made in phenomenological models for high-temperature fatigue (*e.g.*, Refs. 6 through 9). The increase in life with frequency by a factor of 100 occurs under conditions in which creep effects are moderate. Where creep is more significant, an even larger frequency effect will occur.[14] On the other hand, an increase in frequency from 600 to 6×10^4 cpm reduces the fatigue life by a factor of seven, whereas most fatigue models assume an increase in life with frequency. It is also generally assumed, where strain aging doesn't occur, that a reduction in fatigue life occurs at elevated temperature. Table III shows that there is ten-fold increase in fatigue life between room temperature and 1400°F that can be related to the effect of enhanced slip dispersal on crack initiation and Stage I crack propagation. Only at very high frequencies at 1400°F does the fatigue life approach that achieved at room temperature where thermally-activated processes are insignificant, Table III. It has also been shown that large differences in elevated temperature fatigue life can occur under constant test conditions merely because of the presence or absence of suitably oriented microstructural defects.

SUMMARY

The fatigue life of Udimet 700 at 1400°F increases 100-fold with a frequency change from 2 to 600 cpm. At the lowest frequencies, crack initiation occurs at surface-connected grain boundaries and propagation is initially intergranular. With an increase in frequency, intergranular notches produced by oxidation and creep deformation become less important. There is then a transition to subsurface crack initiation at hard phases located at grain boundaries or coherent annealing twin boundary intersections and to Stage I crack propagation.

With an increase in frequency from 600 to 6×10^4 cpm, the fatigue life is reduced by a factor of seven and Stage I remains the predominant mode of cracking. The reduction in life is attributed to the concentration of plastic deformation in fewer and fewer planar bands.

It is likely that the elevated temperature fatigue properties of other engineering materials having a planar slip character will show a similar frequency and temperature dependence and this behavior should be incorporated in the appropriate elevated temperature fatigue models.

ACKNOWLEDGMENTS

We are indebted to Messrs. T. T. Field, S. W. Hopkins, E. D. Johnson, J. J. Nolan and P. D. Retzer for their contribution to the program and to Drs. G. R. Leverant and C. H. Wells for valuable discussions.

REFERENCES

1. N. Stephenson: Memorandum No. M. 320, National Gas Turbine Establishment, Pyestock, Hants, England, June 1958.

2. G. P. Tilly: Current Papers No. 786, Ministry of Aviation, England, December 1963.
3. J. E. Northwood, R. S. Smith and N. Stephenson: Memorandum No. M. 325, National Gas Turbine Engine Establishment, 1959.
4. J. F. Eckel: *Appl. Mater. Res.,* 1965, vol. 4, p. 239.
5. A. Coles, G. J. Hill, R. A. T. Dawson, S. J. Watson: *Thermal and High Strain Fatigue,* p. 270, The Metals and Metallurgy Trust, London, 1967.
6. L. F. Coffin, Jr.: *Fracture 1969,* Proceedings of the Second International Conference on Fracture, p. 643, Chapman and Hall, Ltd., 1969.
7. L. F. Coffin, Jr.: *Proceedings of the Air Force Conference on Fatigue and Fracture of Aircraft Structures and Materials,* Miami Beach, December 1969, in press.
8. S. S. Manson, G. R. Halford, and D. A. Spera: A. E. Johnson Memorial Volume, in press.
9. S. S. Manson: *Exp. Mech.,* 1965, vol. 5, p. 193.
10. E. G. Ellison and C. P. Sullivan: *Am. Soc. Metals, Trans. Quart.,* 1967, vol. 60, p. 88.
11. M. Gell and G. R. Leverant: *Acta Met.,* 1968, vol. 16, p. 553.
12. M. Gell and G. R. Leverant: *Trans. TMS-AIME,* 1968, vol. 242, p. 1869.
13. M. Gell and G. R. Leverant: *Fracture 1969,* Proceedings of the Second International Conference on Fracture, p. 565, Chapman and Hall Ltd., Brighton, England, 1969.
14. M. Gell and G. R. Leverant: MERL, Pratt & Whitney Aircraft, Middletwon, Connecticut, unpublished research, 1970.
15. G. R. Leverant and M. Gell: MERL, Pratt & Whitney Aircraft, Middletown, Connecticut, unpublished research, 1970.
16. F. P. Bullen, A. K. Head, and W. A. Wood: *Proc. Roy. Soc., London,* 1953, vol. 216A, p. 332.
17. W. P. Mason and W. A. Wood: *J. Appl. Phys.,* 1968, vol. 39, p. 5581.
18. W. A. Wood and W. P. Mason: *J. Appl. Phys.,* 1969, vol. 40, p. 4514.
19. C. H. Wells and C. P. Sullivan: *Am. Soc. Metals, Trans. Quart.,* 1964, vol. 57, p. 841.
20. D. J. Duquette, M. Gell, and J. W. Piteo: *Met. Trans.,* 1970, vol. 1, p. 3107.
21. L. H. Burck, C. P. Sullivan, and C. H. Wells: *Met. Trans.,* 1970, vol. 1, p. 1595.